

Influence of heat-treated Cu-Be electrode on machining accuracy in ECMM with Monel 400 alloy

*Original*

Influence of heat-treated Cu-Be electrode on machining accuracy in ECMM with Monel 400 alloy / Liu, Sf; Thangamani, Geethapriyan; Muthuramalingam, T; Shanmugam, R; Ramoni, M. - In: ARCHIVES OF CIVIL AND MECHANICAL ENGINEERING. - ISSN 1644-9665. - 22:4(2022). [10.1007/s43452-022-00478-6]

*Availability:*

This version is available at: 11583/2985223 since: 2024-01-18T14:30:19Z

*Publisher:*

SPRINGER NATURE

*Published*

DOI:10.1007/s43452-022-00478-6

*Terms of use:*

This article is made available under terms and conditions as specified in the corresponding bibliographic description in the repository

*Publisher copyright*

Springer postprint/Author's Accepted Manuscript

This version of the article has been accepted for publication, after peer review (when applicable) and is subject to Springer Nature's AM terms of use, but is not the Version of Record and does not reflect post-acceptance improvements, or any corrections. The Version of Record is available online at: <http://dx.doi.org/10.1007/s43452-022-00478-6>

(Article begins on next page)



# Influence of heat-treated Cu–Be electrode on machining accuracy in ECMM with Monel 400 alloy

Shoufa Liu<sup>1</sup> · T. Geethapriyan<sup>2</sup> · T. Muthuramalingam<sup>3</sup> · Ragavanantham Shanmugam<sup>4</sup> · Monsuru Ramoni<sup>5</sup>

Received: 6 March 2022 / Revised: 17 May 2022 / Accepted: 12 June 2022  
© Wrocław University of Science and Technology 2022

## Abstract

Monel 400 is a nickel–copper alloy utilized in marine and oil refining industries owing to its high corrosion resistance and fire withstanding property. The machining of such higher strength material with complex shapes is possible with electrochemical micromachining (ECMM) process, since it can machine with less wear, better precision, micro-level hole profiles, no heat-affected zone and no thermal stresses. The present study was performed with machining of Monel 400 alloy in ECMM process with copper–beryllium wire electrode under various heat treatments, such as annealing, quenching and normalizing. The lower overcut can be obtained using quenched tool electrode when compared to the other treated tools and untreated tool electrode owing to its fine grain structure which restricts the flow of electrons to side of the tool. The conicity with normalized tool electrode is lower, since it exhibits high electrical conductivity by decreasing the distraction of electrons. Circularity with quenched tool electrode is lower due to its fine grain structure and higher electrical conductivity, since its localization effect increases causing uniform stray current.

**Keywords** Monel · ECMM · Circularity · Conicity · Quenching

## 1 Introduction

Monel 400 is a nickel–copper alloy utilized in marine and oil refining industries owing to its high corrosion resistance and fire withstanding property. It is very tedious to machine since it can be work-hardened very quickly. The unconventional machining processes can easily cut the engineering materials. The laser beam machining (LBM) process can be easily utilized for the machining process. Nevertheless it produces more heat affected zone (HAZ) on the specimens. The abrasive water jet machining (AWJM) process could

produce more taperness during the machining process. The electrical discharge machining (EDM) can remove the material very slowly. Hence, electro-chemical micro-machining (ECMM) can be used for machining Monel 400 alloy. The efficiency of current in electrochemical processing was determined using an electrochemical current determination of HSS from sodium nitrate. The tests are carried out without feeding speed and at several voltages between the electrodes [1]. The different between the electrodes and the electric current is measured with relative to function of time. Dissolution efficiency was determined which was

✉ T. Muthuramalingam  
muthurat@srmist.edu.in; muthu1060@gmail.com

Shoufa Liu  
shoufaliu2000@sina.com

T. Geethapriyan  
devimani.priyan18@gmail.com

Ragavanantham Shanmugam  
rags@navajotech.edu

Monsuru Ramoni  
mramoni@navajotech.edu

<sup>1</sup> School of Mechanical Engineering, Xijing University, Xi'an 710123, People's Republic of China

<sup>2</sup> Department of Mechanical Engineering, SRM Institute of Science and Technology, SRM Nagar, Kattankulathur 603203, India

<sup>3</sup> Department of Mechatronics Engineering, SRM Institute of Science and Technology, SRM Nagar, Kattankulathur 603203, India

<sup>4</sup> Advanced Manufacturing Engineering Technology, School of Engineering, Math and Technology, Navajo Technical University, Crownpoint, NM 87313, USA

<sup>5</sup> Industrial Engineering, School of Engineering, Math and Technology, Navajo Technical University, Crownpoint, NM 87313, USA

influenced by flow rate, electrolyte concentration, electrolyte temperature and current density. The electrochemical micromachining is preferred to other non-conventional machining techniques like laser beam machining, ultrasonic machining, electro-discharge machining are thermal processes and causes excessive deformation on heat affected zones and micro-cracks on the work piece [2]. It was inferred that machining rate could depend on the atomic weight, current and time for dissolution and it does not depends on the hardness and other characteristics of the material. It was discussed about analyzing the influence of parameters like voltage, current, electrolyte concentration, feed rate, flow rate on material removal rate (MRR) and surface roughness ( $R_a$ ) [3]. The machining was performed on SS304 using a copper tool and NaCl electrolyte. Irregular MRR was observed at high current and increase in current results in decrease of surface roughness. As electrolyte flow rate increases, the ion mobility between work piece and electrolyte increases, thus increasing the chemical reaction speed and results in increased MRR. An effort was taken in ECMM of titanium alloy (Ti-6Al-4V) with three different electrolytes concentrations which are capable for drilling accurate micro-holes [4]. The circular cross-sectional hole produced shows very small circularity error using hybrid electrolyte. The ECMM process can be considered to be among the few more effective advanced micro-machining process using which a wide range of applications are calculated. This investigation indicates most predominant parameters like frequency, voltage, duty cycle and electrolyte concentration provide better MRR with low overcut [5]. The ECMM can be used in making advanced and complex shapes in aeronautical industries and its capability to machine macro- and micro-features for biomedical applications [6]. The research and development in the process capabilities, tool, electrolytes and hybrid processes were presented. It was noted that ECM was used to fabricate micro-electrodes and these tools have been used in ECM or EDM processes. The technological advances were studied in electrochemical machining processes [7]. It was concluded that electrolyte concentration and voltage were the most influencing parameter on overcut and material removal rate using gray relational analysis. It was noted that rate of machining and overcut were directly proportional to electrolyte concentration and applied voltage. The experiment analysis was performed in Micro-ECM setup for fabrication of micro-channel in hydrodynamic bearing [8]. It was found that 2 electrolytes, water mixed sodium nitrate and NaOH are used in this experiment to find better results. The current identification method was highlighted to find inter electrode gap characteristics, electrolyte concentration, pulse current and voltage based on model and experiments. A study was performed on the effect

of electrochemical micro-machining process parameters on material removal rate of the  $\alpha$ - $\beta$  titanium alloy (work piece). The process parameters considered were electrolyte concentration, machining voltage and feed rate [9]. An electro-chemical framework was framed with the advancement of smaller scale, miniaturized scaling methods have turned into a hot issue in current industries. The smaller-scale metal opening with high caliber is generally utilized in pieces of center types gear in fields of vitality control, conveying and therapeutic apparatus [10]. It was suggested that the insulated film on silicon-based tool micro-electrodes is a critical process to restrict the stray current and improve the machining localization [11]. As electrolyte flow rate and electrolyte concentration increases, the chemical reaction at the machining area gets speed up and result high material removal rate. From the experiment, it was also observed that the surface roughness and electrolyte concentration are directly proportional to each other [12]. The performance of different sized tool, shape and design in ECMM was studied. Flat, conical with rounded and wedged tool electrodes were used to determine the overcut and material removal rate by various parameters of electrolyte concentration [13]. On heat treating, the grains of the material get altered and thus cause the material to restrict the range of elastic limit in ECM process [14]. The electrical conductivity of the electrode increases due to increase in grain boundaries that restrict the dispersion of ions [15]. A machining was performed on SS304 using a copper tool and NaCl electrolyte in ECMM process. It was found that increase in flow rate of electrolyte increases the MRR, thus increasing the chemical reaction speed between work piece and electrolyte [16]. Genetic algorithm can be used to enhance the ECMM process through optimization [17]. The design of experimentation method could improve the output parameters efficiently by selecting the minimum concentration, voltage, electrode cap and tool feed rate favorable for machining based on various trial and error methods [18]. In ECMM process, duty cycle was the most influencing parameter to contribute material removal rate [19]. The MRR was found to be non-uniform due to increased generation of heat in ECMM process. It can be refined by improving with duty cycle and electrolyte percentage. The tool erosion was observed to reduce with increasing the gram per liter of electrolyte and duty cycle [20].

From the survey, it was inferred that only small amount research works were available to analyze the influence of heat treatment tool electrode in ECMM process. The micro-machining of Monel 400 alloy was not performed considerably. Hence the present investigation was made. The present study was performed with machining of Monel 400 alloy in ECMM process with various heat-treated electrodes.

## 2 Experimental methodology

### 2.1 Selection of workpiece

Monel 400 alloy finds its applications in brine heaters, pumps, propeller shafts, and in other marine applications due to their high corrosion resistant. Monel 400 alloy has high repetitive life cycle and relatively low cost. Monel 400 alloy has good resistance to acids and alkalis. The work piece Monel alloy was selected based on several factors, such as hardness, electrical conductivity, etc., and Monel 400 alloy is stronger than pure nickel. Hence, it was chosen as the workpiece specimen. The dimension of workpiece specimens was chosen as 50 mm × 50 mm with the thickness of 2 mm. The chemical composition consists of iron, copper (cu), nickel (Ni), manganese (Mn), carbon, sulfur and silicon at different percentages by weight shown in Table 1.

### 2.2 Selection of tool electrode

The tool electrodes were selected based upon certain requirements, such as easy fabrication, high electrical conductivity and high corrosion resistance. The tool electrode must possess high wear resistance and have high repetitive cycles. Based on these criteria, copper–beryllium (Cu–Be) has been selected as the tool electrode with the diameter of 0.5 mm. The chemical composition of the electrode is shown in Table 1. The tool electrode was heat-treated into three different methods which are annealing, quenching and normalizing as shown in Fig. 1. The tool electrodes were placed in the muffle furnace and heated up to 790 °C for a time period of 3 h. The copper–beryllium tool electrode pieces are placed in three different containers for three methods of heat treatment (annealing, quenching and normalizing). The heat-treated Cu–Be tool electrode have been directly procured from Mahalakshmi metallurgical corporation, Chennai, India. The heat treatment process takes place in three stages, such as heating period, soaking period and cooling period. In quenching, the heated tool was rapidly quenched by dipping it in water. The tool was kept at room temperature

after heating for normalizing process. Annealing was done by furnace cooling for a time period of 24 h.

### 2.3 ECMM setup

The drilling operations were performed using TTECM-10 ECMM setup manufactured by Sinergy Nano System, India as shown in Fig. 2. ECMM is a controlled process where the material is removed from the metal due to the dissolution of anode in the electrolyte in which the anode is the material to be machined and the cathode is the tool electrode [21]. The electrolyte was supplied to the inner electrode gap (IEG) between the anode and the cathode and the dissolution takes place when current is supplied through the electrodes. The positive current was supplied to the work piece and the negative current is supplied to the tool electrode. It involves the use of a pulsed power supply unit, in which the frequency, duty cycle and voltage can be varied. IEG was maintained less than 50 microns. When the tool and the work piece come into contact, the tool holder returns back to its initial position to prevent electrical component damage. The ECMM setup consists of several components, such as frequency modulator, voltage and current regulator, tool holder, electrolyte filter tank, filter pump and an machining chamber made up of acrylic. The frequency modulator and voltage regulator together makes up the pulsed power supply unit. The frequency and the duty cycle can be varied using the frequency modulator.

### 2.4 Selection of electrolyte

The electrolyte washes away the precipitates that are formed due to the chemical reactions. The electrolytes used in ECMM are passivating and non-passivating electrolytes. Electrolytes are used in ECMM process to fill the IEG between the tool and the work piece by proving free ions to carry the electric current for anodic dissolution. Non-passivating electrolyte was chosen for their aggressive anions. The electrolyte used in the process was Sodium chloride (NaCl)—Analytical reagent grade [22].

**Table 1** Chemical composition of materials

| Workpiece specimen |           |        |        |           |          |         |         |
|--------------------|-----------|--------|--------|-----------|----------|---------|---------|
| Material           | Nickel    | Copper | Iron   | Manganese | Carbon   | Silicon | sulfur  |
| MONEL 400          | 64.95%    | 32.37% | 1.42%  | 0.71%     | 0.0001%  | 0.15%   | 0.010%  |
| Tool               |           |        |        |           |          |         |         |
| Material           | Beryllium |        | Copper | Iron      | Aluminum |         | Silicon |
| Copper Beryllium   | 1.92%     |        | 97.36% | 0.008%    | 0.010%   |         | 0.03%   |

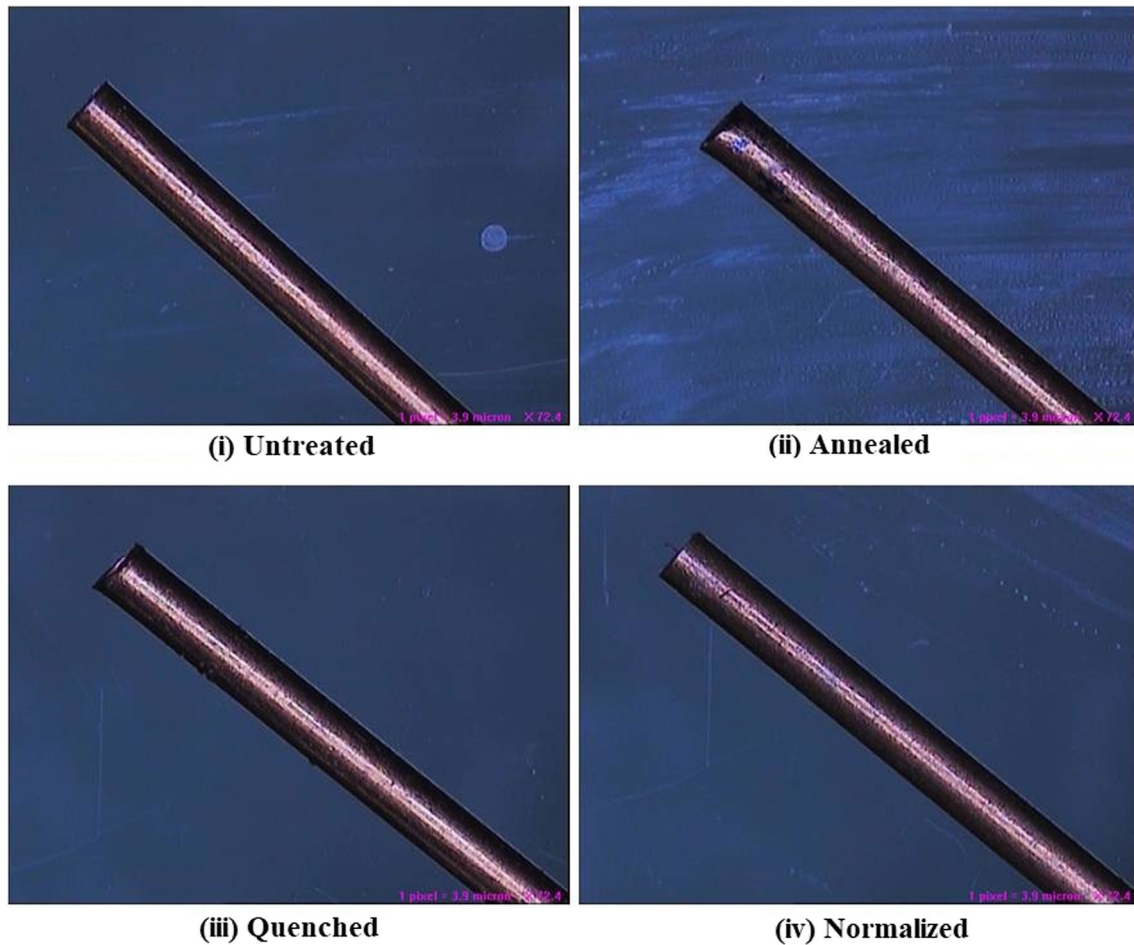


**Fig. 1** Cu-Be tool electrodes used in the present study

## 2.5 Selection of process parameters

The parameters which can be varied are applied voltage (AV), duty cycle (DC), electrolyte concentration (EC) and frequency (F). The electrolyte temperature was maintained to

## 2.6 Measurement of performance measures

Overcut (OC) is defined as the gap formed between the tool electrodes used for machining and the machined hole and denoted in mm.

$$\text{Overcut} = \frac{(\text{Average diameter of the work piece} - \text{External tool diameter})}{2} \quad (1)$$

room temperature. The process variables have been chosen based on the ranges available in ECM setup under higher, medium and lower levels as shown in Table 2 [21, 22]. Since the present study was performed with four factors and three levels with no factors interaction, Taguchi  $L_9$  method was used to generate the value table to get better results [23–25]. All the trials were conducted three times and the average of those experimental values was considered as final response value to enhance the measurement accuracy.

The circularity determines how much each circular section of a cylinder, sphere or cone may deviate from its ideal circular form. The maximum diameter is the circumscribed circle of machined hole and minimum diameter is the diameter of the inscribed circle. It is determined using the vision measuring system and denoted in mm. The machine vision system was measured to measure the circularity using 3 point method—Least Square Method.

**Fig. 2** ECMM process arrangement used in the present study

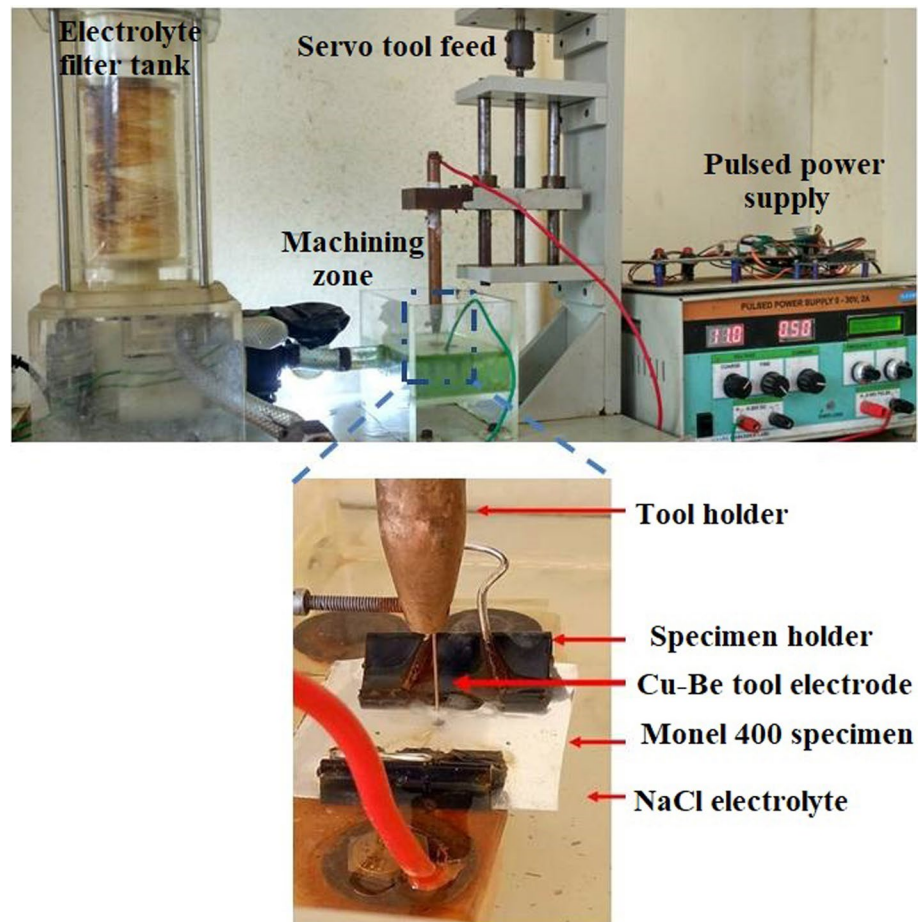


**Table 2** Selection of input parameters

| S.No | Input factors             | Unit | Ranges     |
|------|---------------------------|------|------------|
| 1    | Voltage                   | V    | 10, 12, 14 |
| 2    | Electrolyte concentration | g/l  | 20, 25, 30 |
| 3    | Frequency                 | Hz   | 50, 60, 70 |
| 4    | Duty cycle                | %    | 33, 50, 66 |

$$\text{Circularity error} = (\text{Minimum circumscribing circle} - \text{Maximum inscribing circle}) \quad (2)$$

The conicity defines how much a cylindrical profile varies from an ideal cylinder and denoted in mm.

$$\text{Conicity} = \frac{\text{Diameter at entry} - \text{Diameter at exit}}{2 \times \text{hole thickness}} \quad (3)$$

### 3 Results and discussion

#### 3.1 Surface morphology of heat-treated Cu-Be tool electrode

Heat treatment of Cu-Be tool electrode above 790 °C causes the beryllium in Cu-Be to dissolve in the alpha solid solution phase and on rapid quench, it maintains beryllium in solid state. Figure 3 shows the surface morphology image of the annealed tool electrode before heat treatment, after heat treatment and after machining. From these surface morphology images, it can be seen that after heat treatment the cracks on the surface of tool gets reduced and formation of uniform surface throughout. The grain size can be modified in the annealed specimen due to low rate of cooling which leads to relieve the internal stress and causing the tool electrode to become soft.

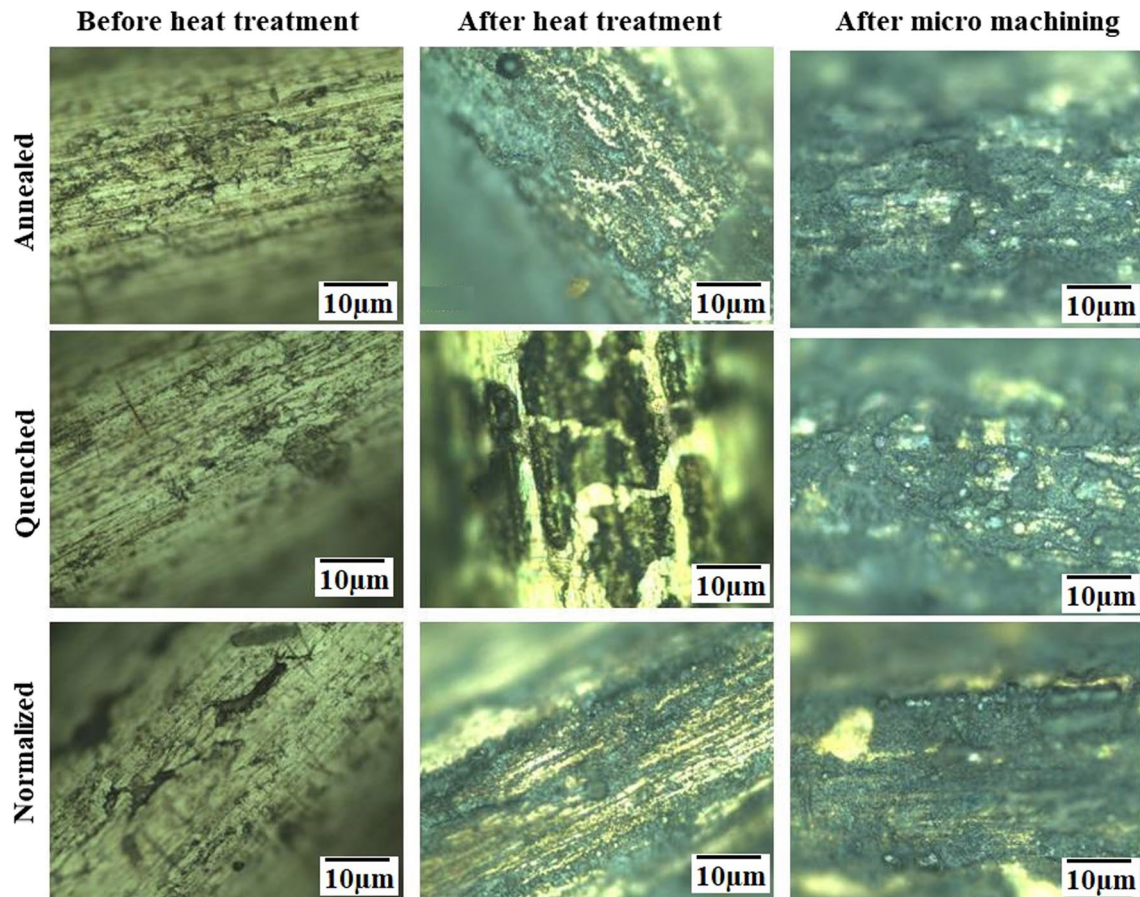


**Fig. 3** Surface Morphology of tool electrodes under heat treatment

In quenching heat treatment process the specimen is heated up to 790 °C with the soaking time of 2 h and it differs from other heat treatment process by the method of cooling. In quenching the specimen is rapid cooled by dipping the specimen in the brine solution (salt water). Quenching heat treatment process increases the growth of grain boundaries and thus causing fine grain structure. Figure 3 shows the surface morphology image of the quenched tool electrode before heat treatment, after heat treatment and after machining. From the surface morphology image, it can be observed that after heat treatment process the crack on surface gets reduced. In the after machining surface morphology image, more pits and pores can be observed this is due to the interchange of the ions from the tool to the work piece.

Normalized heat treatment process is similar to the other heat treatment processes which differ by the method the cooling. In normalizing process the specimen is allowed to cool in the normal atmospheric temperature. In after heat treatment surface morphology image, occurrence of pit and cracks were observed. This was due to the reduction of the pitting resistance owing to the exposure of material to the atmosphere during cooling. In the after machining surface

morphology image, it was observed that more electron discharge occurred from the crack and pits.

### 3.2 Electrical conductivity analysis of heat-treated Cu–Be Tool electrode

The electrical conductivity of the electrode can determine the machinability in ECMM process. It was determined using desktop multi-meter. It can be observed that the conductivity of the tool electrode got increased after the heat treatment process. It was also observed that the conductivity

**Table 3** Conductivity of the tool electrodes under heat treatment

| Heat treatment  | Conductivity ( $\Omega^{-1}/\text{mm}$ ) |                 |
|-----------------|--|-----------------|
|                 | Before machining                         | After machining |
| Untreated tool  | 36.63                                    | 3.90            |
| Annealed tool   | 32.12                                    | 2.7             |
| Quenched tool   | 37.06                                    | 4.21            |
| Normalized tool | 36.94                                    | 3.01            |

of the quenched tool electrode was greater among all other tool electrode. This is because of the effect of heat treatment where the grain structures gets altered and increase in the growth of grain boundaries. Due to more grain boundaries the electron distraction gets reduced thus results in increased conductivity.

From Table 3, it was observed that the conductivity of annealed tool was least among the four tool electrodes. The migration of atoms in the crystal lattice occurs which increases the ductility and decreases hardness, thereby reducing the conductivity in the tool electrode. In ECMM process, the machining measures may be affected by the electrical conductivity of the tool electrode. The electrical conductivity of the tool may be affected with the heat treatment, since the electrical resistance is proportional to the change in temperature owing to the migration of atoms in

the crystal lattice. The conductivity value after machining gets drastically reduced due to the higher temperature of the tool electrode caused during machining. With increase in temperature, the electrical resistance of metal gets increases thus causes the atoms to vibrate and collide with moving electrons. Hindrance of moving electrons reduces the conductivity of tool electrode.

### 3.3 Influence of process parameters on overcut

Figure 4 shows electrolyte concentration was the most influencing parameter for the normalized tool electrode where the overcut decreases with increase in the electrolyte concentration. Maximum overcut is obtained at 25 g/l while minimum overcut is obtained at 30 g/l. When supplied voltage passes through tool electrode, it tends to form a stray current around

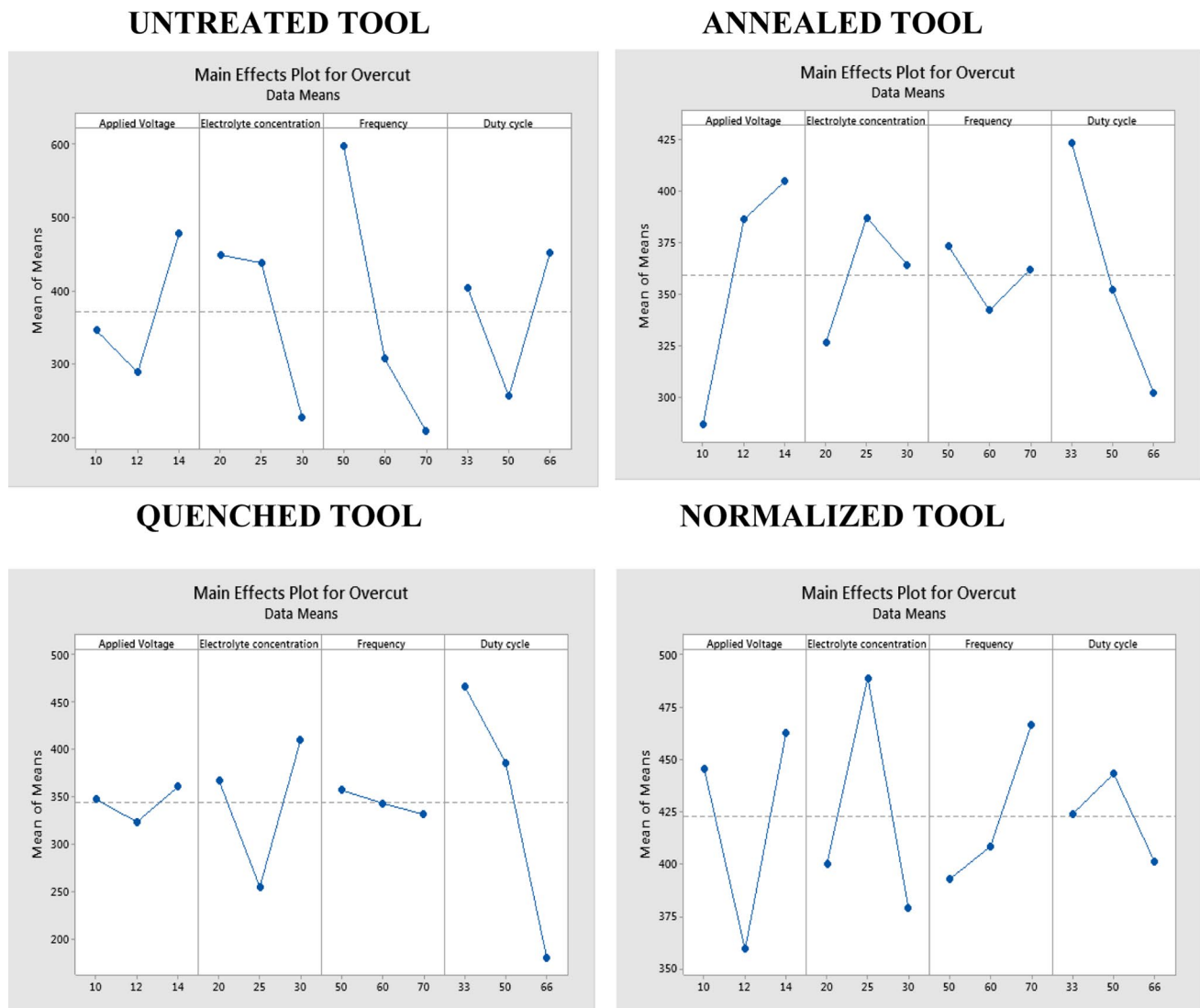


Fig. 4 Main effect plot for overcut

the tool electrode. Since the size of the bubble formed is small, the stray current machines more material around the hole. In case of higher electrolyte concentration, the size of bubble formed is large which blocks the stray current thus results in low overcut. In case of the untreated tool electrode, it is inferred that the frequency is the most influencing parameter where the overcut decreases with increase in the frequency. This was due to generation of high frequency pulses per unit time than the low frequency pulses. This leads to increase of localization with decrease in the stray current which results in low overcut.

Duty cycle shows the most deviation for annealing and quenched tool electrode. It was observed that the increase in the duty cycle leads to the decrease in overcut. In case of the heat-treated tool electrode the conductivity is affected thereby restricting the dispersion of electrons, thus increase the localization effect. In ECM process, the machining measures may be affected by the electrical conductivity of the tool electrode. As you aware, the electrical conductivity of the tool may be affected with the heat treatment, since the electrical resistance is proportional to the change in temperature owing to the migration of atoms in the crystal lattice. So that, during load-on time in high duty ratio the rate of dissolution of ions is greater in the localized area thereby decrease in overcut. Using different input parameters, the work pieces were machined and

were analyzed using machine vision measurement system. For overcut, when the duty cycle is at 66% and lesser the applied voltage results in better overcut for all the tool electrodes. The overcut is poor when the duty cycle is at 33% and also when the applied voltage is high. Therefore, the increase in applied voltage and decreased duty cycle leads to the increase in overcut as shown in Fig. 5 using vision measuring system (VMS). Untreated tool electrode possesses the maximum overcut among the four tool electrodes.

It can be inferred that the normalized tool has the least overcut as shown in Table 4. It was observed that the overcut of quenched tool is 3.65% lesser than untreated tool. This was due to the fine grain structure which could restrict the flow of electrons to side of the tool. Thus the current available at the frontal gap between the work piece and tool get increased. Also it was observed that the normalized tool has the highest overcut among the four tools. It has 19.73% higher than untreated tool and annealed tool has 4.06% higher than untreated tool.

### 3.4 Influence of process parameters on conicity

For quenched tool and normalized tool electrode the most influential parameter was electrolyte concentration as shown in Fig. 6. The maximum and minimum conicity were

Fig. 5 VMS image for Overcut

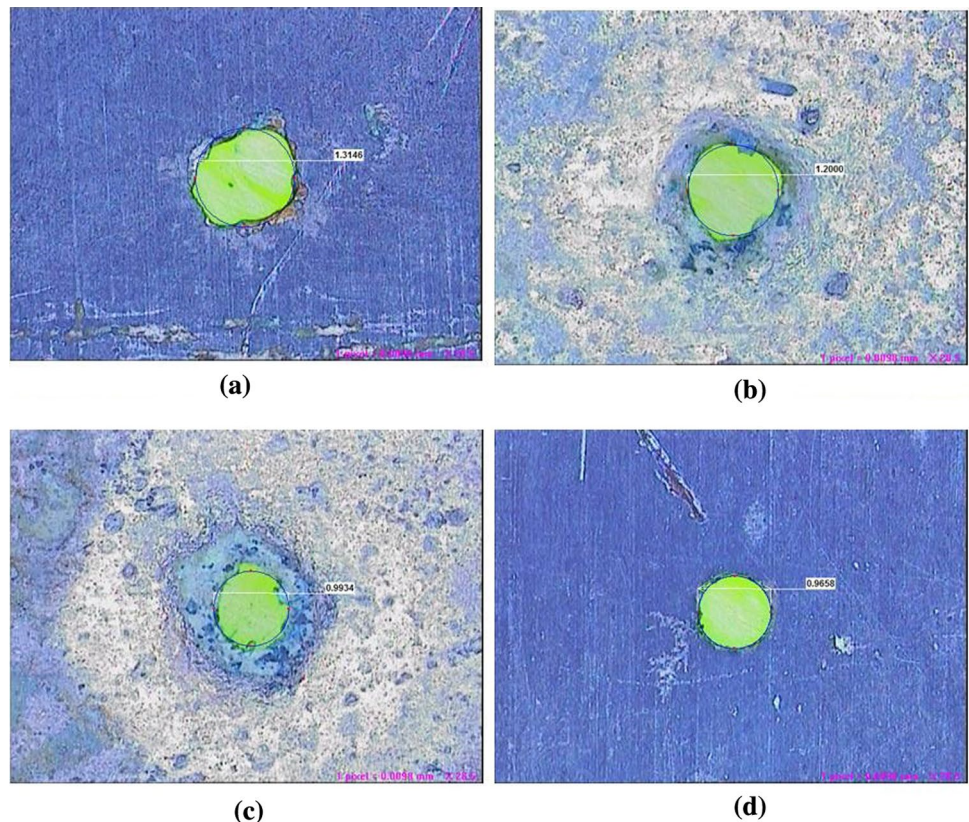


**Table 4** Effect of heat-treated tools on overcut

| S.no | Voltage (v) | Electrolyte con-<br>centration (g/l) | Frequency<br>(Hz) | Duty<br>cycle (%) | Overcut        |               |               |                 |
|------|-------------|--------------------------------------|-------------------|-------------------|----------------|---------------|---------------|-----------------|
|      |             |                                      |                   |                   | Untreated tool | Annealed tool | Quenched tool | Normalized tool |
|      |             |                                      |                   |                   | (mm)           |               |               |                 |
| 1    | 10          | 20                                   | 50                | 33                | 0.6842         | 0.3325        | 0.5058        | 0.3947          |
| 2    | 10          | 25                                   | 60                | 50                | 0.2342         | 0.2908        | 0.2996        | 0.5181          |
| 3    | 10          | 30                                   | 70                | 66                | 0.1202         | 0.2376        | 0.2367        | 0.4246          |
| 4    | 12          | 20                                   | 60                | 66                | 0.3842         | 0.2796        | 0.1819        | 0.301           |
| 5    | 12          | 25                                   | 70                | 33                | 0.2263         | 0.4812        | 0.3445        | 0.4707          |
| 6    | 12          | 30                                   | 50                | 50                | 0.2562         | 0.3981        | 0.4443        | 0.3063          |
| 7    | 14          | 20                                   | 70                | 50                | 0.2799         | 0.3679        | 0.4133        | 0.505           |
| 8    | 14          | 25                                   | 50                | 66                | 0.8543         | 0.3899        | 0.1211        | 0.4775          |
| 9    | 14          | 30                                   | 60                | 33                | 0.3045         | 0.4565        | 0.5481        | 0.4064          |

obtained at 20 g/l and 25 g/l respectively. This was because at low concentration the bubbles formed during machining are smaller which allow the side current to machine out more material resulting high conicity. When electrolyte concentration was high the bubbles formed were large and this vacuum space block the side current from machining more material from the work piece resulting to a low conicity.

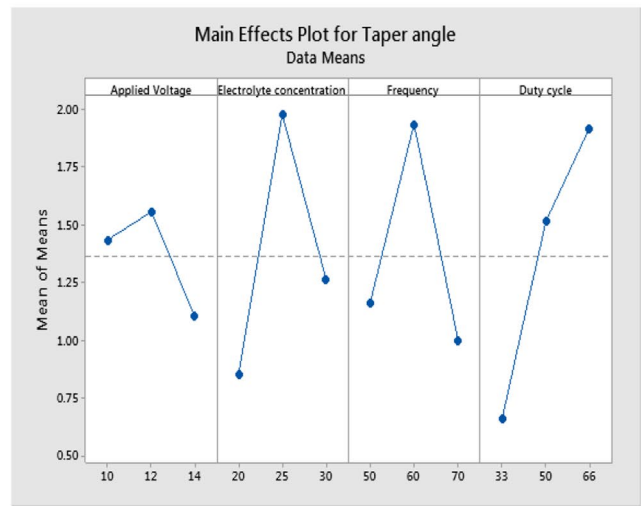
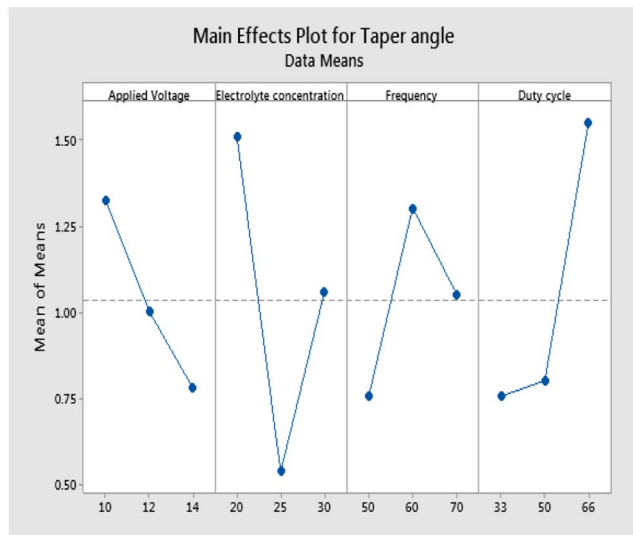
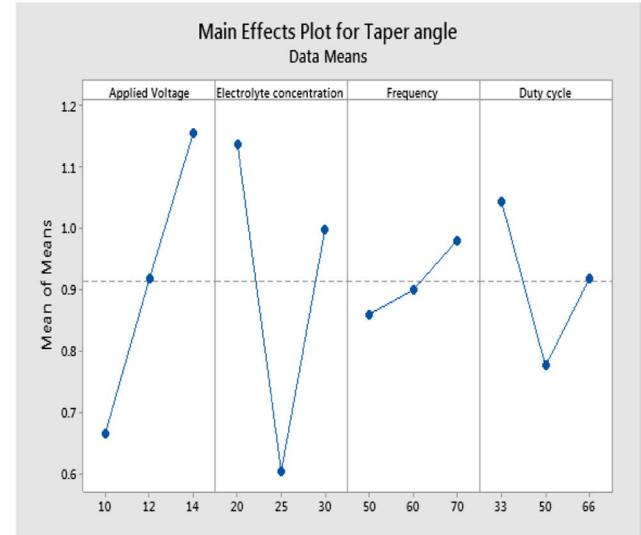
In the case of untreated tool, it was inferred that the duty cycle was the most influencing parameter for the conicity. From the graph, it can be observed that the conicity increases with increase in the duty cycle ratio. Minimum conicity obtained for the duty ratio 50% and maximum at 66% duty ratio. This is because at 66% the pulse-on time is more compared to pulse-off time. Due to less pulse-off time the removed material or sludge which formed were not washed or flushed away fully and the by-products start to clog to the electrode thus produces spark due to which more material is removed hence by minimizing these around the machining area reduces conicity. In the case of annealed tool electrode, it was inferred that the frequency was the most influencing parameter for the conicity. From the graph, it can be inferred that the maximum conicity is obtained at 60 Hz and minimum conicity at 70 Hz. An increase in frequency implies a decrease in pulse duration. It was also noted that the duty cycle ratio is also high when frequency is high. This results in lower as faster removal of material takes place.

By using different input parameters, the work piece was machined and analyzed. The lower applied voltage and frequency could reduce the conicity. When the applied voltage was 10 V, the conicity was lesser for normalized tool and annealed tool. When the applied voltage was 12 V and the duty cycle was 33%, the conicity was lower for untreated and quenched tool electrode as shown in Table 5. The increase in frequency results in increasing the conicity of the untreated and annealed tool electrodes. However with quenched tool electrode, the increase in duty cycle leads to poor conicity.

It can be inferred that the normalized tool has the less conicity. This was because the heat-treated tool electrode exhibits high conductivity by decreasing the dislocation of electrode thus results in faster rate of machining reduces conicity. It was found that the conicity of normalized tool is 28.65% and quenched tool is 19.05% lesser than untreated tool. Annealed tool has the highest conicity among the four tools. Annealed tool has 6.61% higher conicity than untreated tool.

### 3.5 Influence of process parameters on circularity at entry

From the Fig. 7, it was inferred that the frequency was the most influencing parameter for circularity at entry. As the frequency increases, the circularity error at entry gets decreased. The increase in frequency implies a decrease in pulse duration and an increase in the ionization which improves the circularity. Better results are obtained when the circularity error was minimum. It was observed that the electrolyte concentration was the most influencing parameter for the annealed tool electrode. Also as the applied voltage increases, the circularity error decreases. When the electrolyte concentration is less, then the ionization rate is reduced in annealed tool which in turn increases the circularity of the hole machined. In case of quenched tool electrode, applied voltage is the most influencing parameter. As the applied voltage increases, the circularity error gets decreased. When the voltage is high the amount of current passing through the electrode is high which means that the stray current through the sides of the tool is high and uniform, resulting to low circularity error of the hole machined. In case of normalized tool electrode, electrolyte concentration is the most influencing parameter. An increase in electrolyte concentration results in the increase of circularity error. The circularity error is minimum at lower concentration. Also the circularity error reduces with increase in applied voltage. When the electrolyte concentration is high, the number of ions

**UNTREATED TOOL****ANNEALED TOOL****QUENCHED TOOL****NORMALIZED TOOL****Fig. 6** Main effect plot for conicity

available for dissolution is higher which results in non-uniform distribution of ions, thereby increasing circularity error.

Using different input parameters, the work piece was machined and was analyzed using VMS as shown in Fig. 8. For the annealed, quenched and normalized tool electrodes, greater the applied voltage and lesser the electrolyte concentration lead to lower circularity error at entry as shown in Table 6. The lower applied voltage and electrolyte concentration leads to poor circularity error at entry. For untreated tool electrode, it was just an opposite way. The lower applied voltage could reduce the circularity error. Whereas the higher applied voltage could increase the circularity error. It can be inferred that the quenched tool has the least circularity error with 39.57%

lesser than the untreated tool electrode. Quenched tool has fine grain structure which when subjected to high applied voltage possess uniform dissolution. Thus it could result on reducing circularity error than the other tool electrode. The annealed tool electrode has 1.36% lesser circularity error than untreated tool electrode and normalized tool has 2.8% lesser circularity error than the untreated tool electrode.

### 3.6 Influence of process parameters on circularity at exit

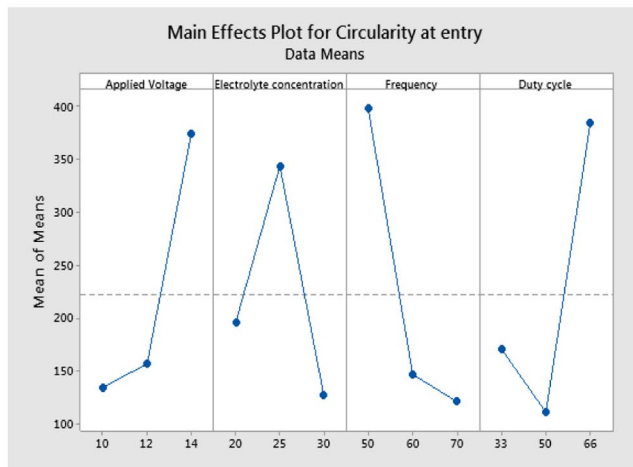
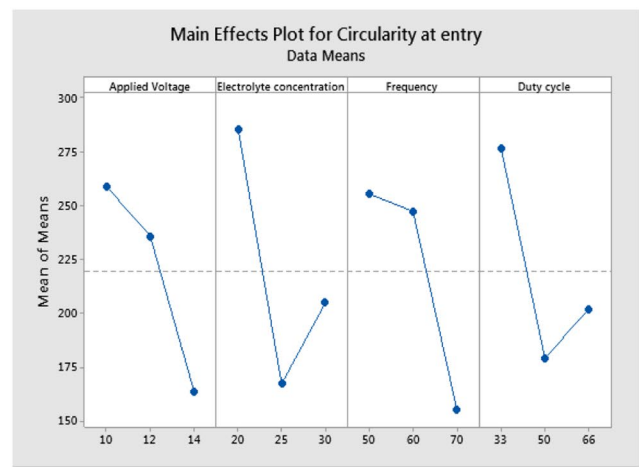
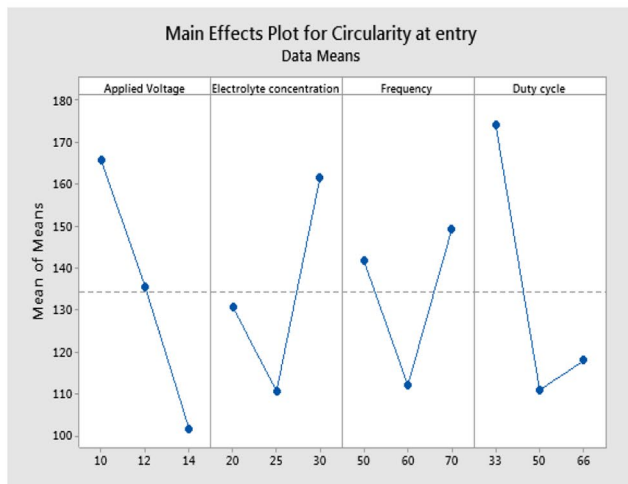
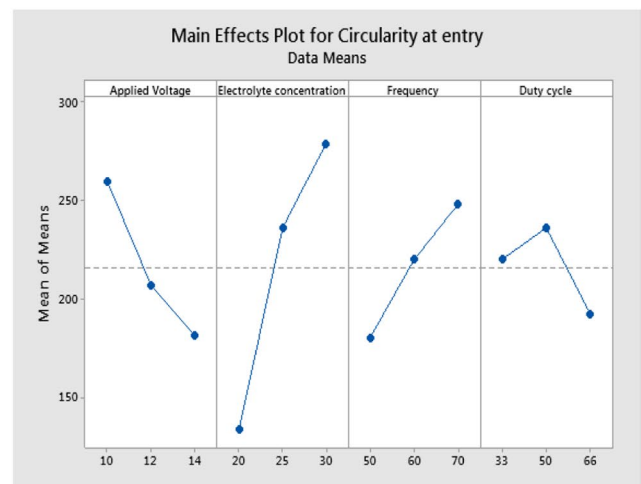
From Fig. 9, it was inferred that the frequency was the most influencing parameter for the circularity at exit for untreated

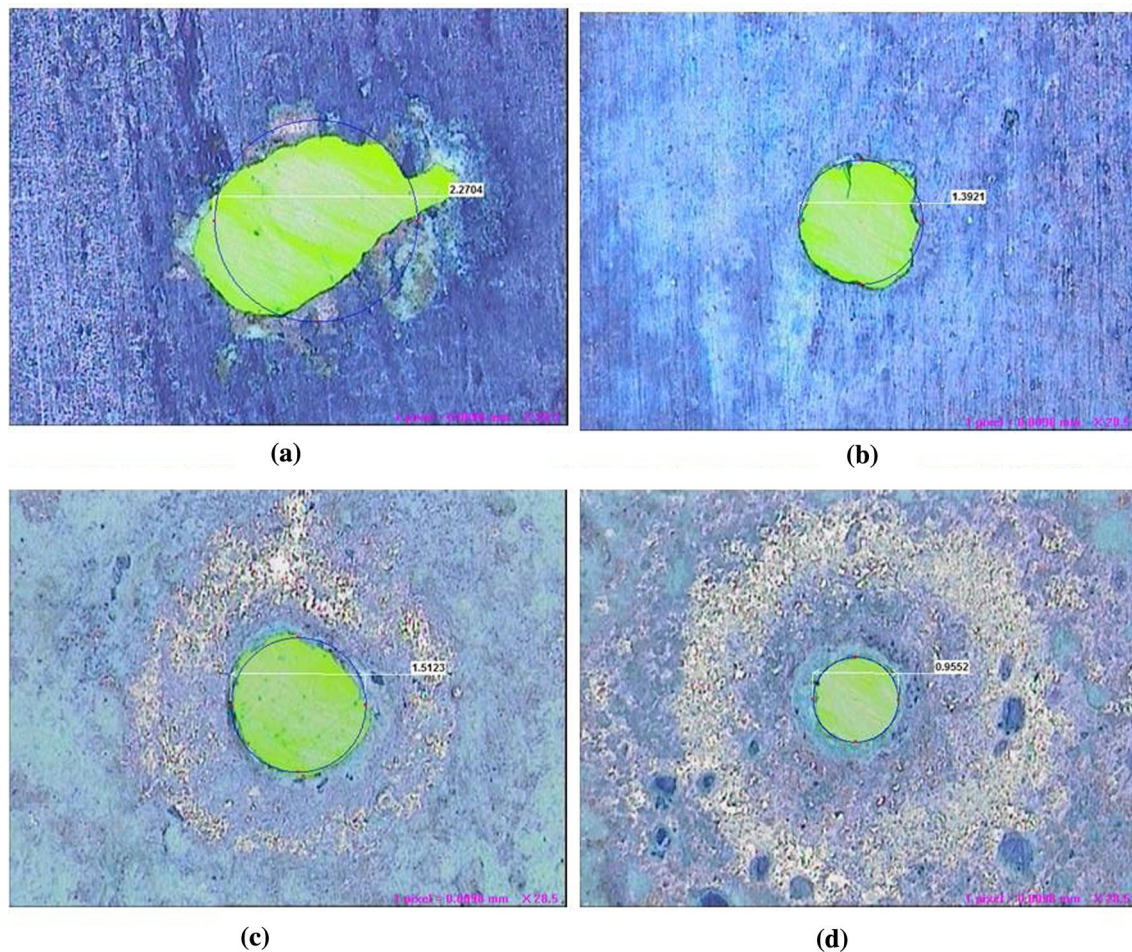
**Table 5** Effect of heat-treated tools on conicity

| S.no | Voltage (v) | Electrolyte concentration (g/l) | Frequency (Hz) | Duty cycle (%) | Conicity       |               |               |                 |
|------|-------------|---------------------------------|----------------|----------------|----------------|---------------|---------------|-----------------|
|      |             |                                 |                |                | Untreated tool | Annealed tool | Quenched tool | Normalized tool |

|   |    |    |    |    |        |        |        |       |
|---|----|----|----|----|--------|--------|--------|-------|
| 1 | 10 | 20 | 50 | 33 | 0.2635 | 0.0114 | 1.24   | 0.968 |
| 2 | 10 | 25 | 60 | 50 | 1.0827 | 2.77   | 0.86   | 0.206 |
| 3 | 10 | 30 | 70 | 66 | 1.329  | 1.523  | 1.88   | 0.825 |
| 4 | 12 | 20 | 60 | 66 | 1.9415 | 2.17   | 2.26   | 1.134 |
| 5 | 12 | 25 | 70 | 33 | 2.679  | 1.099  | 0.24   | 0.808 |
| 6 | 12 | 30 | 50 | 50 | 0.189  | 1.4    | 0.5099 | 0.813 |
| 7 | 14 | 20 | 70 | 50 | 0.813  | 0.378  | 1.036  | 1.31  |
| 8 | 14 | 25 | 50 | 66 | 2.525  | 2.067  | 0.515  | 0.8   |
| 9 | 14 | 30 | 60 | 33 | 0.704  | 0.8708 | 0.79   | 1.36  |

**UNTREATED TOOL****ANNEALED TOOL****QUENCHED TOOL****NORMALIZED TOOL****Fig. 7** Main effect plot for circularity at entry



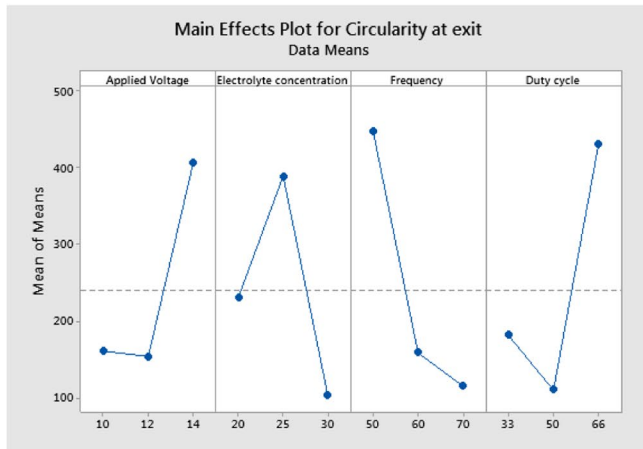
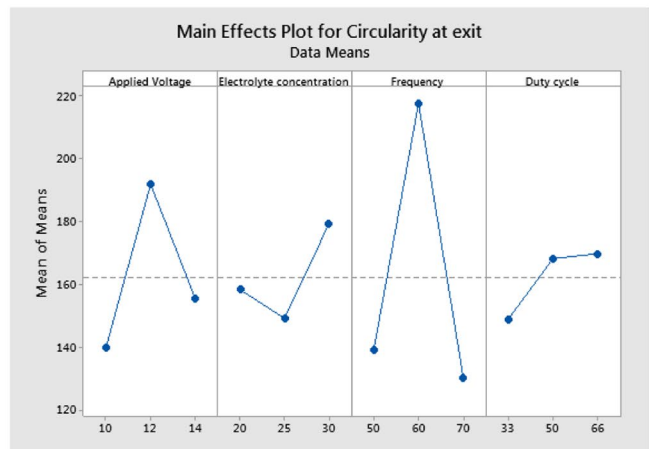
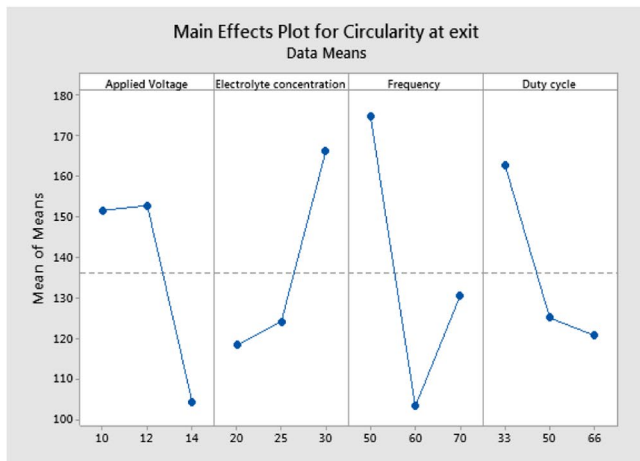
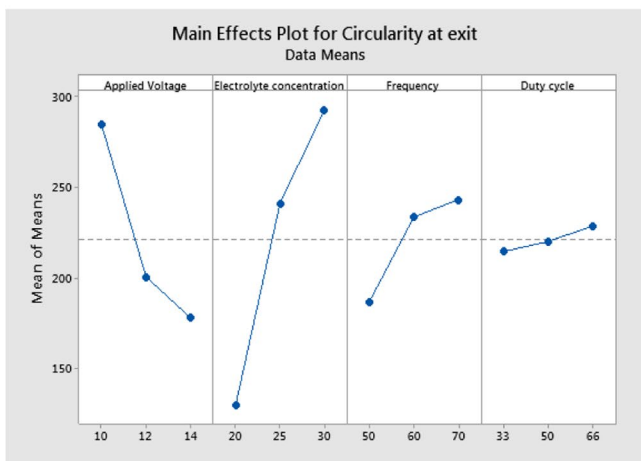
**Fig. 8** VMS image for circularity at entry

**Table 6** Effect of heat-treated tools on circularity at entry

| S.no | Voltage (v) | Electrolyte con-<br>centration (g/l) | Frequency<br>(Hz) | Duty<br>cycle (%) | Circularity error at entry |               |               |                 |
|------|-------------|--------------------------------------|-------------------|-------------------|----------------------------|---------------|---------------|-----------------|
|      |             |                                      |                   |                   | Untreated tool             | Annealed tool | Quenched tool | Normalized tool |
|      |             |                                      |                   |                   | (mm)                       |               |               |                 |
| 1    | 10          | 20                                   | 50                | 33                | 0.2337                     | 0.4187        | 0.2094        | 0.1453          |
| 2    | 10          | 25                                   | 60                | 50                | 0.0699                     | 0.1949        | 0.0964        | 0.3035          |
| 3    | 10          | 30                                   | 70                | 66                | 0.1004                     | 0.163         | 0.1915        | 0.331           |
| 4    | 12          | 20                                   | 60                | 66                | 0.2186                     | 0.3128        | 0.0934        | 0.1042          |
| 5    | 12          | 25                                   | 70                | 33                | 0.1264                     | 0.1774        | 0.1666        | 0.2629          |
| 6    | 12          | 30                                   | 50                | 50                | 0.1267                     | 0.2173        | 0.1469        | 0.2542          |
| 7    | 14          | 20                                   | 70                | 50                | 0.1372                     | 0.1256        | 0.0896        | 0.1506          |
| 8    | 14          | 25                                   | 50                | 66                | 0.8352                     | 0.1301        | 0.069         | 0.1414          |
| 9    | 14          | 30                                   | 60                | 33                | 0.1531                     | 0.2342        | 0.1465        | 0.2519          |

tool electrode. As the frequency increases, the time duration of power supply was increased. It could lead to produce the uniform hole throughout the work piece, thus resulting in lower circularity error at the exit. In case of annealed tool

electrode, frequency was the most influencing parameter for the circularity at exit. The circularity at exit increases for frequency at 50 Hz and again reduces at 66 Hz, whereas it constantly decreases for increase in duty cycle. The increased

**UNTREATED TOOL****ANNEALED TOOL****QUENCHED TOOL****NORMALIZED TOOL****Fig. 9** Main Effect Plot for circularity at entry

duty cycle refers to increased pulse on time. The increased frequency helps in flushing of the slurry formed during the operation, which results in uniform machining of hole throughout. In case of quenched tool electrode, frequency was the most influencing parameter for the circularity at exit. Also as the applied voltage increases, the circularity error at exit decreases. The higher the voltage supplied to the tool, the uniform machining taking places throughout the process with sufficient ions present to pass the electric current. The presence of more ions than required tends to increase the circularity error. As the electrolyte concentration increases, the circularity error also tends to increase. In case of normalized tool electrode, electrolyte concentration is the most influencing parameter for the circularity at exit. Also in this tool electrode, the increase in duty cycle and frequency also results in increase in circularity error at exit. The increase in applied voltage results in decrease in circularity error. The presence of sufficient voltage supply

and required ions results in uniform machining throughout the hole which results in lesser circularity error. The lower electrolyte concentration and higher applied voltages could result in lower circularity error at exit for quenched, normalized and annealed tool electrodes. For untreated tool electrode, the greater the electrolyte concentration, the better the circularity error at exit. The higher duty cycle with lower applied voltage has resulted in higher circularity error at the exit for quenched, normalized and annealed tool electrodes. The increase in voltage and duty cycle caused a poor circularity error at exit in the untreated tool electrode.

From Table 7, it can be inferred that the quenched tool has the lower circularity error at exit. The quenched tool has 43.41% lower circularity error than the untreated tool electrode. The untreated tool electrode has the highest circularity error among the four electrodes. The annealed tool has 32.56% lesser and normalized tool has 8.12% lower circularity error at exit than the untreated tool electrode. The

**Table 7** Effect of Heat-Treated Tools on circularity at exit

| S.no | Voltage (v) | Electrolyte concentration (g/l) | Frequency (Hz) | Duty cycle (%) | Circularity at exit |               |               |                 |
|------|-------------|---------------------------------|----------------|----------------|---------------------|---------------|---------------|-----------------|
|      |             |                                 |                |                | Untreated tool      | Annealed tool | Quenched tool | Normalized tool |
|      |             |                                 |                |                | (mm)                |               |               |                 |
| 1    | 10          | 20                              | 50             | 33             | 0.2998              | 0.0991        | 0.1989        | 0.1522          |
| 2    | 10          | 25                              | 60             | 50             | 0.096               | 0.1879        | 0.0954        | 0.3166          |
| 3    | 10          | 30                              | 70             | 66             | 0.0872              | 0.1322        | 0.1605        | 0.3865          |
| 4    | 12          | 20                              | 60             | 66             | 0.2519              | 0.2508        | 0.0864        | 0.1291          |
| 5    | 12          | 25                              | 70             | 33             | 0.1171              | 0.1334        | 0.1617        | 0.2361          |
| 6    | 12          | 30                              | 50             | 50             | 0.0926              | 0.1917        | 0.2103        | 0.2368          |
| 7    | 14          | 20                              | 70             | 50             | 0.1412              | 0.1253        | 0.0695        | 0.1074          |
| 8    | 14          | 25                              | 50             | 66             | 0.9533              | 0.1265        | 0.1154        | 0.1708          |
| 9    | 14          | 30                              | 60             | 33             | 0.1279              | 0.2144        | 0.128         | 0.2555          |

quenched tool electrode has fine grain structure and good conductivity values even after machining. It could lead to uniform machining throughout the process for reducing the circularity error at exit.

## 4 Conclusion

In the present study, Monel 400 alloy was machined using ECM process parameters with untreated and various heat-treated tool electrodes. The input characteristics, such as applied voltage, electrolyte concentration, frequency and duty cycle, were varied suitably to get the optimum values of response parameters like overcut, conicity and circularity. From the experimental investigations carried out using untreated and heat-treated tool electrodes, the following conclusions have been drawn.

- The lower overcut can be obtained using quenched tool electrode when compared to the other treated tools and untreated tool electrode owing to its fine grain structure which restricts the flow of electrons to side of the tool.
- The conicity is better with normalized tool electrode, since it exhibits high electrical conductivity by decreasing the distraction of electrons.
- The circularity is better with quenched tool electrode due to its fine grain structure and higher electrical conductivity, since its localization effect increases causing uniform stray current.

**Acknowledgements** Not applicable.

**Author contributions** All authors are involved in conducting experiments, analysis, data interpretation, finding and manuscript preparation.

**Funding** There is no funding involved in this study.

**Availability of data and material** Not applicable.

**Code availability** Not applicable.

## Declarations

**Conflicts of interest/Competing interests** There are no conflicts of interest in this study.

**Ethics approval** Not applicable.

**Consent to participate** Not applicable.

**Consent for publication** Not applicable.

## References

1. Zhang A, Xu Z, Lu J, Wang Y. Improvement of blade platform accuracy in ECM utilizing an auxiliary electrode. *Mater Manuf Process*. 2020;35:951–60. <https://doi.org/10.1080/10426914.2020.1752920>.
2. Geethapriyan T, Kalaichelvan K, Muthuramalingam T. Multi performance optimization of electrochemical micro-machining process surface related parameters on machining Inconel 718 using Taguchi-grey relational analysis. *Metall. Ital.* 2016;4: 13–19. [http://www.aimnet.it/la\\_metallurgia\\_italiana/2016/aprile/Muthuramalingam.pdf](http://www.aimnet.it/la_metallurgia_italiana/2016/aprile/Muthuramalingam.pdf). Accessed 30 Apr 2022.
3. Zhao Z, Ma Z, Liu Y, Wu X, Guo H. Optimization and affections of cathode feed angle on machining accuracy error distribution of aero-engine blade in electrochemical machining. *Key Eng Mater.* 2018;764:225–34. <https://doi.org/10.4028/www.scientific.net/KEM.764.225>.
4. Geethapriyan T, Muthuramalingam T, Moiduddin K, Mian SH, Alkhalefah H, Umer U. Performance analysis of electrochemical micro machining of titanium (Ti-6Al-4V) alloy under different electrolytes concentrations. *Metals*. 2021;11:247. <https://doi.org/10.3390/met11020247>.

5. Liu Y, Li M, Niu J, Lu S, Jiang Y. Fabrication of taper free micro-holes utilising a combined rotating helical electrode and short voltage pulse by ECM. *Micromachines*. 2019;10(1):28. <https://doi.org/10.3390/mi10010028>.
6. Zhang H, Liu S, Yue W, Xiao H, Zhang P. Experimental study of surface characteristic in electrochemical machining of 35CrMo steel. *Metals*. 2018;8(7):509. <https://doi.org/10.3390/met8070509>.
7. Liu Y, Huang SF. Experimental study on electrochemical drilling of micro holes with high aspect ratio. *Adv Mater Res*. 2014;941–944:1952–5. <https://doi.org/10.4028/www.scientific.net/AMR.941-944.1952>.
8. Dong S, Wang Z, Wang Y. Research on micro-EDM with an auxiliary electrode to suppress stray-current corrosion on C17200 beryllium copper alloy in deionized water. *Int J Adv Manuf Technol*. 2017;93:857–67. <https://doi.org/10.1007/s00170-017-0478-8>.
9. Geethapriyan T, Kalaichelvan K, Muthuramalingam T, Rajadurai A. Performance analysis of process parameters on machining  $\alpha$ - $\beta$  titanium alloy in electrochemical micromachining process. *Proc Inst Mech Eng B J Eng Manuf*. 2018;232:1577–89. <https://doi.org/10.1177/0954405416673103>.
10. Wang Y, Chen H, Wang Z, Zhou Z, Shan D. Development of a soft-computer numerical control system for micro-electrochemical machining. *Am J Nanotechnol*. 2010;1:51–5. <https://doi.org/10.3844/ajnsnp.2010.51.55>.
11. Yong L, Di Z, Yongbin Z, Shaofu H, Hongbing Y. Experimental investigation on complex structures machining by electrochemical micromachining technology. *Chin J Aeronaut*. 2010;23:578–84. [https://doi.org/10.1016/S1000-9361\(09\)60257-0](https://doi.org/10.1016/S1000-9361(09)60257-0).
12. Saranya S, Sankar AR. Fabrication of precise microchannels using a side-insulated tool in a spark assisted chemical engraving process. *Mater Manuf Process*. 2018;33(13):1422–8. <https://doi.org/10.1080/10426914.2017.1401728>.
13. Thanigaivelan R, Arunachalam RM. Experimental study on the influence of tool electrode tip shape on electrochemical micromachining of 304 stainless steel. *Mater Manuf Process*. 2010;25:1181–5. <https://doi.org/10.1080/10426914.2010.508806>.
14. Millett JCF, Whiteman G, Park NT, Case S, Thomas GA. The effects of heat treatment upon the shock response of a copper-beryllium alloy. *Acta Mater*. 2019;165:678–85. <https://doi.org/10.1016/j.actamat.2013.01.021>.
15. Goel H, Pandey PM. Experimental investigations into the ultrasonic assisted jet electrochemical micro-drilling process. *Mater Manuf Process*. 2017;32(13):1547–56. <https://doi.org/10.1080/10426914.2017.1279294>.
16. Uttarwar SS, Chpde IK. Experimental study of effect of parameter variation on output parameters for electrochemical machining of SS AISI 202. *IOSR. J Mech Civ Eng*. 2013;5(5): 65–71. <https://www.iosrjournals.org/iosr-jmce/papers/vol5-issue5/H0556571.pdf>. Accessed 30 Apr 2022.
17. Krishnan R, Duraisamy S, Palanisamy P, Veeramani A. Optimization of the machining parameters in the electrochemical micro-machining of nickel. *Mater Technol*. 2018;52:253–8. <https://doi.org/10.17222/mit.2017.045>.
18. Das MK, Kumar K, Barman TK, Sahoo P. Optimization of surface roughness and MRR in electrochemical machining of EN31 tool steel using grey-Taguchi approach. *Procedia Manuf Sci*. 2014;6:729–40. <https://doi.org/10.1016/j.mspro.2014.07.089>.
19. Saravanan D, Arularasu M, Ganesan K. A study on electrochemical micromachining of super duplex stainless steel for biomedical filters. *ARN J Eng Appl Sci*. 2012;7(5):517–23. [http://www.arnjournals.com/jeas/research\\_papers/rp\\_2012/jeas\\_0512\\_684.pdf](http://www.arnjournals.com/jeas/research_papers/rp_2012/jeas_0512_684.pdf). Accessed 30 Apr 2022.
20. Paul L, Hiremath SS. Response surface modelling of micro holes in electrochemical discharge machining process. *Procedia Eng*. 2013;64:1395–404. <https://doi.org/10.1016/j.proeng.2013.09.221>.
21. Shanmugam R, Ramoni M, Geethapriyan T, Muthuramalingam T. Influence of additive manufactured stainless steel tool electrode on machinability of beta titanium alloy. *Metals*. 2021;11:778. <https://doi.org/10.3390/met11050778>.
22. Geethapriyan T, Muthuramalingam T, Kalaichelvan K. Influence of process parameters on machinability of Inconel 718 by electrochemical micromachining process using TOPSIS technique. *Arab J Sci Eng*. 2019;44:7945–55. <https://doi.org/10.1007/s13369-019-03978-5>.
23. Muthuramalingam T, Vasanth S, Vinothkumar P, Geethapriyan T, Rabik MM. Multi criteria decision making of abrasive flow oriented process parameters in abrasive water jet machining using Taguchi–DEAR methodology. *SILICON*. 2018;10:2015–21. <https://doi.org/10.1007/s12633-017-9715-x>.
24. Thangaraj M, Akash R, Krishnan S, Phan NH, Pi VN, Elsheikh AH. Surface quality measures analysis and optimization on machining titanium alloy using CO<sub>2</sub> based Laser beam drilling process. *J Manuf Process*. 2021;62:1–6.
25. Muthuramalingam T, Moiduddin K, Akash R, Krishnan S, Mian SH, Ameen W, Alkhalefah H. Influence of process parameters on dimensional accuracy of machined Titanium (Ti-6Al-4V) alloy in Laser Beam Machining Process. *Opt Laser Technol*. 2020;132:106494.

**Publisher's Note** Springer Nature remains neutral with regard to jurisdictional claims in published maps and institutional affiliations.